DEVELOPMENT OF A GENERAL HYBRID FINITE-DIFFERENCE TIME-DOMAIN / METHOD OF MOMENTS (FDTD/MOM) COMPUTATIONAL ELECTROMAGNETICS TECHNIQUE

Dimitra I. Kaklamani[1], Codruta Vancea[2], Florin Vancea[3] and Nikolaos K. Uzunoglu[1]

[1]Department of Electrical and Computer Engineering
National Technical University of Athens
9 Iroon Polytechniou Street, Zografos 15780, Athens, Greece

[2]Department of Electrical Engineering, University of Oradea
5 Armatei Romane Street, 3700 Oradea, Bihor, Romania

[3]Department of Computer Science, University of Oradea
5 Armatei Romane Street, 3700 Oradea, Bihor, Romania

Abstract

A new hybrid Computational Electromagnetic technique is presented based on combined use of Finite-Difference Time-Domain (FDTD) and Method of Moments (MoM) technique. MoM is employed to determine the current distribution on perfect conductors and to satisfy the exact boundary conditions on the interface of inhomogeneous field penetrable material media by solving a Kirchhoff type integral equation, while FDTD is employed to describe the electric field inside the field penetrable regions. The case of two dimensional analysis is presented, while the suitability of the proposed technique to treat arbitrary structures in terms of their shape and constituents is exhibited.

1. INTRODUCTION

During the last 20 years a large amount of research work has been carried out in applying the Finite-Difference Time-Domain (FDTD) technique to treat various electromagnetic (EM) structures, by making use of the Yee's [1] algorithm. Various type of Absorbing Boundary Conditions (ABC's) simulating the radiation conditions at infinity have been employed to truncate the region being discretized, within which the field is computed in a nodal mesh.

Despite the very high versatility of FDTD in treating many practical problems, there is still a drawback related to the ABC; that is the truncation of the region within which the field is computed. Despite many efforts, this generic problem remains an open issue. The same problem exists in using the Finite Element (FE) technique, where this «truncation problem» has been successfully faced by using an integral equation (IE) formulation to implement the radiation conditions.

In this context, a new hybrid approach is presented in this article based on the combination of the Method of Moments (MoM) [2] and the FDTD [1,3]. The

motivation in proposing this technique is based on the fact that, although MoM is highly successful in solving arbitrary shaped conducting objects, the FDTD technique is the most versatile method in treating arbitrary shaped, inhomogeneous, dispersive and anisotropic lossy dielectric materials. Therefore, the complementarity of the two techniques is used to propose a general computational EM solver.

In the following, the case of two dimensional (2D) fields with a single electric field component and non-dispersive media is presented. However, the proposed method is general and is being extended to three dimensional (3D) - vector field and dispersive media structures.

2. COMBINATION OF FDTD AND MOM

Consider the structure presented in Fig. 1. A field penetrable region characterized by a dielectric permittivity ε(x,y), a magnetic permeability μ(x,y) and a conductivity σ(x,y) -all three time independent functions- and a perfect electric conductor (PEC)

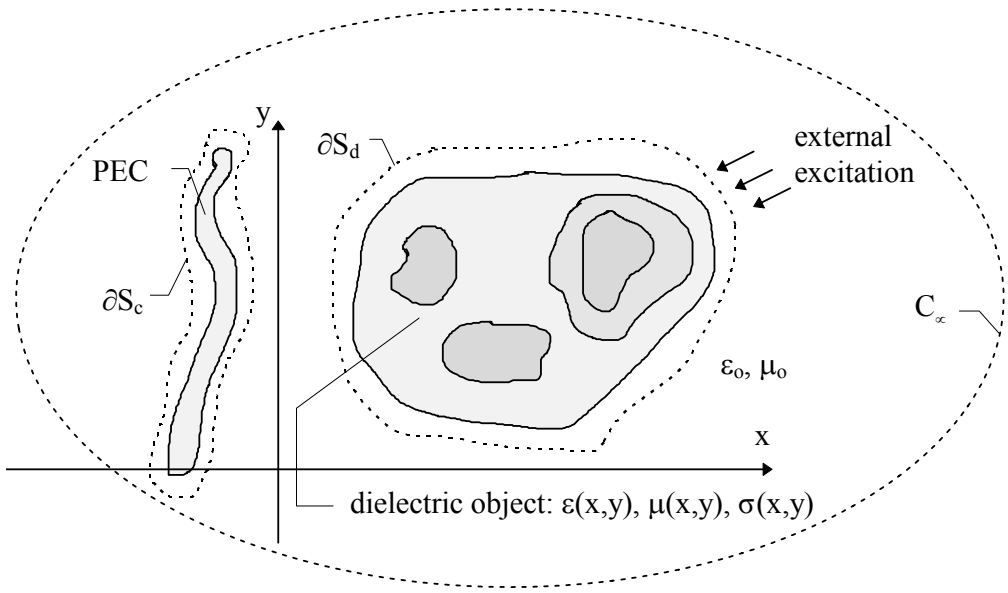

Figure 1. Generalized 2D scattering geometry.

are assumed to be placed in the free space. The electric field is taken to be

$$\underline{E}(\underline{\rho}, t) = \hat{z}\Psi(\underline{\rho}, t) \tag{1}$$

where $\underline{\rho} = x\hat{x} + y\hat{y}$ and t is the time variable. The arbitrary external excitation primary field -either an incident plane wave or a near field source- is described in terms of a known field function $\Psi_0(\underline{\rho}, t)$.

Applying the Green's theorem for the free space region bounded by the curves ∂S_d, ∂S_c and C_∞ (infinite radius circle), a time domain integral equation is easily obtained [4] in terms of the surface electric fields $\Psi(\underline{\rho},t)$, as

$$\Psi(\underline{\rho},t) = \Psi_0(\underline{\rho},t) + \int_{-\infty}^{+\infty} dt' \int_{\partial S_c+\partial S_d} d\ell' \left(G(\underline{\rho}|\underline{\rho}'|t-t') \frac{\partial \Psi(\underline{\rho}',t')}{\partial n} - \frac{\partial G(\underline{\rho}|\underline{\rho}'|t-t')}{\partial n} \Psi(\underline{\rho}',t') \right) \quad (2)$$

where $\frac{\partial}{\partial n}$ denotes the normal derivative, $\underline{\rho},\underline{\rho}' \in (\partial S_c \vee \partial S_d)$, $d\ell'$ is the elementary arc length and

$$G(\underline{\rho}|\underline{\rho}'|t-t') = \frac{H\left(t-|\underline{\rho}-\underline{\rho}'|/c\right)}{\sqrt{t^2-|\underline{\rho}-\underline{\rho}'|^2/c^2}} \quad (3)$$

is the free space 2D time dependent Green's function, with

$$H(\xi) = \begin{cases} 1 & \text{for } \xi > 0 \\ 0 & \text{for } \xi \le 0 \end{cases} \quad (4)$$

being the Heaviside function, $|\underline{\rho}-\underline{\rho}'| = \sqrt{(x-x')^2+(y-y')^2}$ and $c = 1/\sqrt{\varepsilon_0\mu_0}$ being the speed of the EM radiation in vacuum.

Eq. (2) is solved via a MoM and a collocation technique. The integrations along both the boundary curves ∂S_d and ∂S_c and the time axis are discretized, as

$$\Psi(\underline{\rho}_i,t_m) = \Psi_0(\underline{\rho}_i,t_m) + \sum_{k=1}^{m} \int_{(k-1)\Delta t}^{k\Delta t} dt' \sum_{j=1}^{N_c+N_d} \Delta\ell' \left(G(\underline{\rho}_i|\underline{\rho}'_j|t_m-t') \frac{\partial \Psi(\underline{\rho}'_j,t')}{\partial n} - \frac{\partial G(\underline{\rho}_i|\underline{\rho}'_j|t_m-t')}{\partial n} \Psi(\underline{\rho}'_j,t') \right) \quad (5)$$

where $t_m = m\Delta t$ (m=1, 2, …) are the field measurement time instants, N_c and N_d are the number of discrete points on ∂S_d and ∂S_c respectively, while $\underline{\rho}_1$, $\underline{\rho}_2$, …, $\underline{\rho}_{N_c}$, $\underline{\rho}_{N_c+1}$, …, $\underline{\rho}_{N_c+N_d}$ are the position vectors on the boundary curves. Furthermore, the normal derivative $\partial\Psi/\partial n$ is computed by taking points on and in the ∂S_d and ∂S_c curves. Then, the inner to ∂S_d points, i.e. the points within the dielectric object region are linked to an FDTD modal mesh (see the next sub-section), while the PEC condition $\Psi=0$ is employed on (and in) ∂S_c.Following a lengthy analysis, the time integrals at the right hand side of eq. (5) are computed in terms of the time instants prior to the field measurement time instant at the left hand side (i.e. t_m in eq. (5)). Therefore, starting at t=0, when the incident field Ψ_0 has not yet arrived to either of the dielectric

or conducting objects, and being $\Psi(\underline{\rho},t)\big|_{t=0} = 0$, the electric fields on the ∂S_d and ∂S_c boundary curves are computed, taking always into account the link with the field inside the dielectric object.

To this end, adopting a square nodal mesh inside the dielectric object and discretizing also the time axis, a recursive FDTD equation can be written, as [5]

$$\Psi^{n+1}(i,j) = -\Delta t\frac{\sigma(i,j)}{\varepsilon(i,j)}\Psi^{n+1/2}(i,j) + \frac{1}{\mu(i,j)\varepsilon(i,j)}\left(\frac{\Delta t}{\Delta x}\right)^2\left(\Psi^n(i+1,j)+\Psi^n(i-1,j)\right)$$
$$+\frac{1}{\mu(i,j)\varepsilon(i,j)}\left(\frac{\Delta t}{\Delta y}\right)^2\left(\Psi^n(i,j+1)+\Psi^n(i,j-1)\right) + \Delta t\frac{\sigma(i,j)}{\varepsilon(i,j)}\Psi^{n-1/2}(i,j) - \Psi^{n-1}(i,j)$$
$$+2\left(1-\frac{1}{\mu(i,j)\varepsilon(i,j)}\left(\frac{\Delta t}{\Delta x}\right)^2-\frac{1}{\mu(i,j)\varepsilon(i,j)}\left(\frac{\Delta t}{\Delta y}\right)^2\right)\Psi^n(i,j) \qquad (6)$$

where $\Psi^n(i,j)$ is the field at the time instant $t_n=n\Delta t$ (n=1, 2, …) and at the nodal point (i,j), Δt is the time increment and $\Delta x=\Delta y=\Delta s$ is the lattice space increment common in the x- and y-coordinate directions. Following the standard FDTD procedure, eq. (6) is used with a time step procedure to determine the field inner to the dielectric object.

In the case of abrupt discontinuities of the $\varepsilon(i,j)$, $\mu(i,j)$ and $\sigma(i,j)$ parameters, a mesh deformation technique is employed to satisfy the boundary condition and the corresponding derivatives in eq. (6) are accordingly modified. In order to achieve numerical stability, the Curant criterion $c\Delta t \le \Delta s/\sqrt{2}$ [6] is always satisfied.

The fields on the ∂S_d boundaries are linked with the nodal points just within the dielectric object. Through this link and the time step procedure of both eqs (5) and (6), the field distribution $\Psi(\underline{\rho},t)$ is obtained along the time axis. Note that, the fact that the boundary curves ∂S_d and ∂S_c can be taken exactly on the surfaces of the dielectric and conducting bodies minimizes the number of nodes used to describe the field.

3. NUMERICAL RESULTS

The method described in sec. 2 is employed to compute the structure shown in Fig. 2, where the inhomogeneous dielectric object/cylinder is enclosed in a rectangular

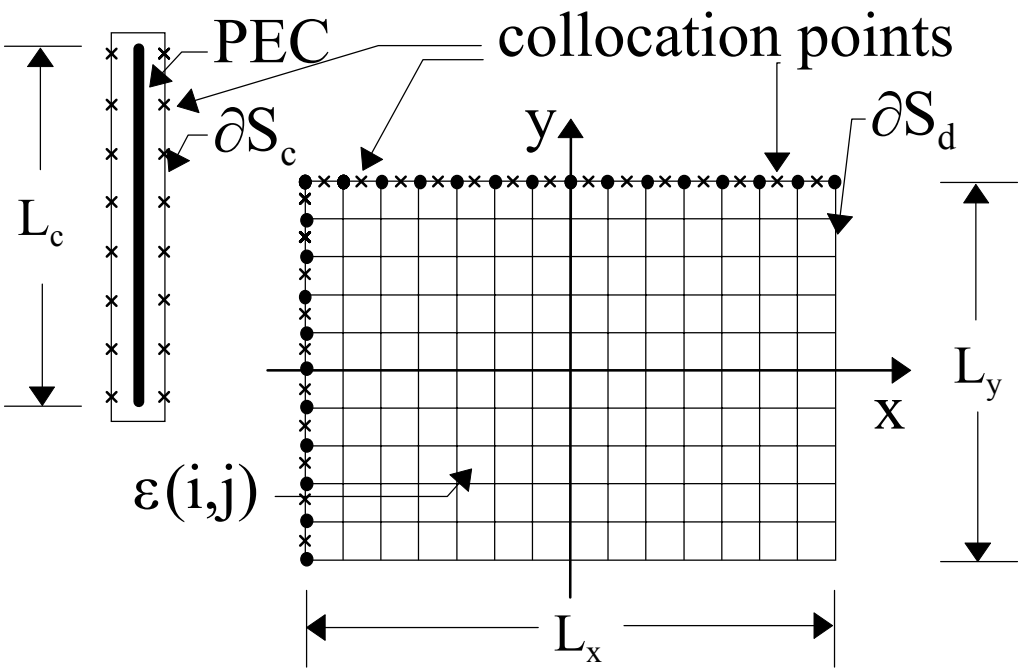

Figure 2. Numerical computation geometry.

FDTD grid of dimensions $L_x \times L_y$, while the conductor is taken be of strip shape with zero thickness and width L_c. In solving eq. (5), on ∂S_d the mid points between the FDTD scheme points are taken as collocation points to discretize the Green's function equation. The incident field $\Psi_0(\underline{\rho}, t)$ is simulated by a time pulse, as

$$\Psi_0(\underline{\rho}, t) = p\left(t - t_0 - \frac{x\cos\alpha + y\sin\alpha}{c}\right) \tag{7}$$

where $$p(\xi) = \begin{cases} 1 & \text{for } 0 < \xi < \tau \\ 0 & \text{otherwise} \end{cases} \tag{8}$$

α is the angle of incidence and $t_0>0$ is taken sufficiently large, so that at t=0 the Ψ_0 is zero on both ∂S_d and ∂S_c. Also, the pulse duration τ is taken to be much larger than Δt.

Numerical computations have been carried out for an incident pulse with τ=4 nsec and α=45°. The conducting strip of width L_c=1.9 m with its centre at (x=-30, y=0). Stability tests have been carried out by varying all the spatial and incremental quantities and the accuracy of the results in terms of convergence is observed and verified. In Fig. 3 indicative numerical results are shown for diverse discretization schemes (varying both $\Delta s=\Delta\ell$ space increment and Δt time increment) for the case of

a rectangular dielectric cylinder of dielectric permittivity ε_r=10 placed at the centre of an FDTD grid with L_x=2.9 m and L_y=1.9 m. The accuracy is of course expected to grow worse as time increases, due to error accumulation.

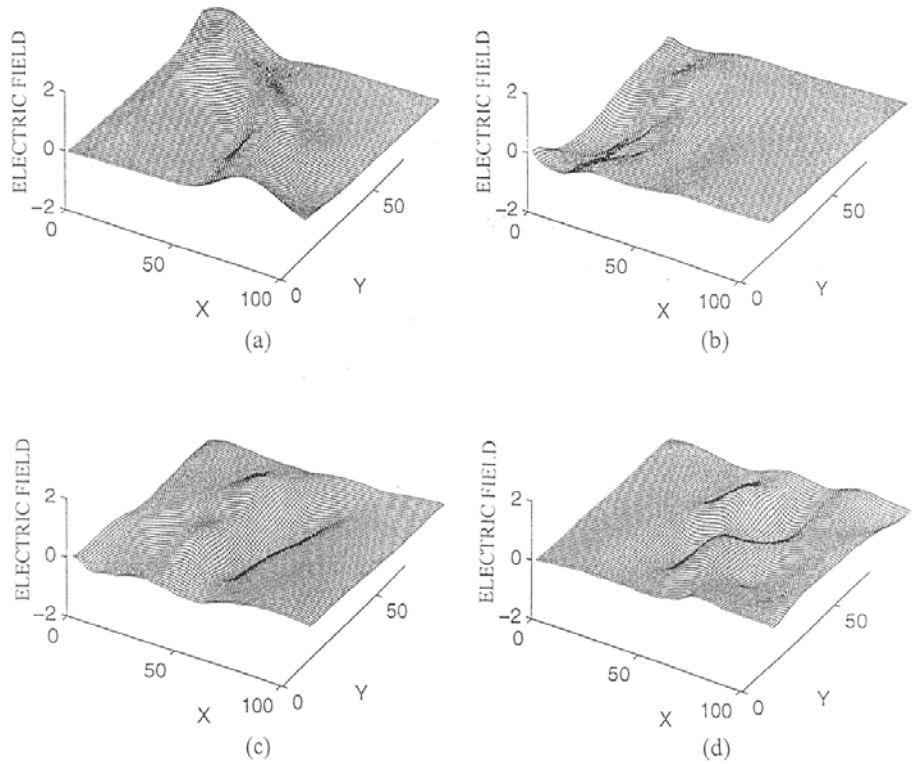

Fig. 3. Convergence pattern: referring to Fig.2, the centre of the L_c=1.9 m width conducting strip is at (x=-30, y=0) and a rectangular dielectric cylinder of ε_r=10 is placed at the centre of the FDTD grid with L_x=2.9 m and L_y=1.9 m, while for the incident pulse it is τ=4 ns and α=45° and the simulation time is t=30.0 ns (the first-order reflected by the strip waves cross the dielectric region).
(a) $\Delta t=12\times10^{-11}$ $\Delta\ell=\Delta s=0.1$ (b) $\Delta t=8\times10^{-11}$ $\Delta\ell=\Delta s=0.1$ (c) $\Delta t=12\times10^{-11}$ $\Delta\ell=\Delta s=0.08$ (d) $\Delta t=8\times10^{-11}$ $\Delta\ell=\Delta s=0.08$

Presentation of the numerical results by using advanced visualization techniques proved to be highly useful to ensure the accuracy of the proposed technique, by observing the validity of fundamental laws of electromagnetism, such as that of reflection and diffraction of EM waves by the conductor and the dielectric medium, or the disappearance of reflected by the mesh edges waves, when there is no dielectric (just free space) inside ∂S_d. In Fig. 4, a sample case is shown for the structure examined in Fig. 3 and for four different time instants, starting from a time instant when the incident pulse propagates for the first time through the dielectric region (Fig. 4(a)), going to a time instant when the pulse reaches the conducting strip (Fig. 4(b)), then to a time instant when reflections from the strip start to appear (Fig. 4(c))

and finally to a time instant when the reflected by the strip waves cross the dielectric region (Fig. 4(d)). More results concerning different dielectric permittivity values, dielectric cylinder shapes and excitation pulses are available at the web site http://www.cc.ece.ntua.gr/~fvancea. The satisfaction of the boundary conditions at each time step, as well as the observed propagation phenomena prove the validity of the derived numerical results.

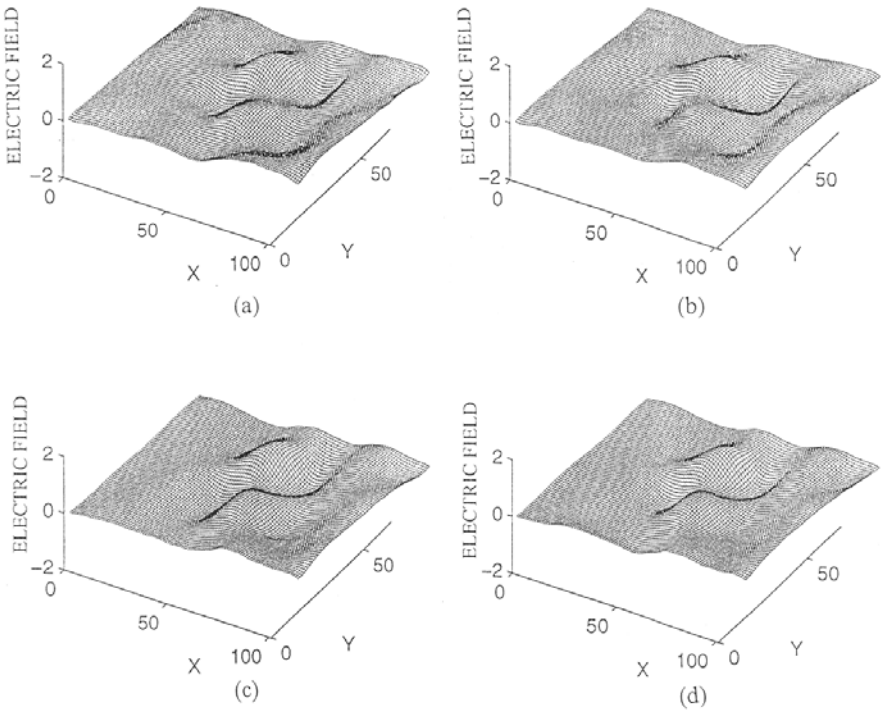

Figure 4. Scattering phenomena: the scattering structure of Fig.3 at four different time instants ($\Delta t=12\times10^{-11}$, $\Delta\ell=\Delta s=0.08$).
(a) t=8.4 ns (b) t=16.4 ns (c) t=22.4 ns (d) t=30.0 ns

4. CONCLUSION - FUTURE WORK

A novel hybrid computational EM technique based on the combined use of MoM and FDTD has been described for the case of 2D structures. Although in the present paper the case of dispersionless materials is considered, the proposed approach is easily extendible to dispersive materials, by taking into account the convolution integrals connecting the field quantities. Presently, the method is extended to 3D - full vector field case structures. The developed method has been proved to be highly efficient and accurate, since no «Artificial» ABC is imposed to truncate the field around the scatterers and the radiation conditions are embedded with the IE formulation.

REFERENCES

[1] K.S. Yee, «Numerical solution of initial boundary value problems involving Maxwell's equations in isotropic media,» *IEEE Trans. Antennas Propagat.,* vol. AP-14, pp. 302-307, 1966.

[2] R.F. Harrington, *Field Computation by Moment Methods*. New York: Macmillan, Florida: Krieger Publishing, 1983.

[3] A. Taflove, *Computational Electrodynamics: The Finite-Difference Time-Domain Method.* Norwood, MA, Artech House, 1995.

[4] D.S. Jones, *Theory of Electromagnetism*. Oxford: Pergamon Press, 1964.

[5] A. Taflove, «Review of the formulation and applications of the Finite-Difference Time-Domain method for numerical modeling of electromagnetic wave interactions with arbitrary structures,» *Wave Motion,* vol. 10, no. 6, pp. 547-582, 1988.

[6] A. Taflove and M.E. Brodwin, «Numerical solution of steady-state electromagnetic scattering problems using the time-dependent Maxwell's equations,» *IEEE Trans. Microwave Theory Tech.,* vol. MTT-23, pp. 623-630, 1975.